Int. J. Nano Dimens., 12 (3): 203-210, Summer 2021

ORIGINAL ARTICLE

Green synthesis of Silver and Silver-gold core-shell nanoparticles using Pineapple leaf extract (Ananas comosus) and study of their antibacterial properties

***Debashish Acharya*[1,*], *Bidhan Mohanta*[1], *Piyush Pandey*[2]**

[1] *Department of Physics, Assam University, Silchar, Assam, 788011, India*
[2] *Department of Microbiology, Assam University, Silchar, Assam, 788011, India*

Received 19 August 2020; revised 22 February 2021; accepted 06 March 2021; available online 10 March 2021

Abstract

The advantage of using plants and plant metabolites over expansive and toxic chemical methods for nanoparticles (NPs) synthesis has fascinated researchers to investigate the mechanisms of bio-reduction of metal ion for various biomedical applications. Herein, pineapple leaf extract was used for the synthesis of silver (Ag) and bimetallic silver-gold (Ag-Au) core-shell NPs which offered an economic and sustainable synthetic route compared to toxic chemical method. The synthesized NPs were further subjected to UV-visible spectrometer to investigate the formation kinetics at specific time intervals. To reveal the presence of various functional groups in the leaf extract responsible for bio-reduction of Ag ions and subsequent formation of core-shell nanostructure, FTIR study was conducted. Morphology and structural properties were examined by TEM and XRD. Further, disc diffusion test was employed to reveal the antibacterial effectiveness of NPs against Gram-positive (*Staphylococcus aureus*) and Gram-negative (*Escherichia coli*) bacteria. The study revealed that both Ag and Ag-Au NPs are good antibacterial candidates and bacterial sensitivity to NPs was found to vary depending on bacterial species.

Keywords: *Ag-Au; Antibacterial; Core-Shell; Disk-Diffusion; Green Synthesis; Pineapple.*

How to cite this article

Acharya D., Mohanta B., Pandey P. Green synthesis of Silver and Silver-gold core-shell nanoparticles using Pineapple leaf extract (Ananas comosus) and study of their antibacterial properties. Int. J. Nano Dimens., 2021; 12(3): 203-210.

INTRODUCTION

Nanotechnology has been becoming a rapidly growing technology in modern research broadly dealing with design, synthesis, and manipulation of particle structure ranging from 1-100 nm [1-3]. Since its emergence, the technology has been rapidly gaining importance in a number of areas such as health care, food, cosmetics, drug-gene delivery, chemical industries, electronics, space industries, energy science, optoelectronic devices, single- electron transistors, and photo electrochemical applications [4-7]. With the advancement of nanotechnology, researchers are now able to develop complex hybrid structures like core-shell, multi shell, hollow shell which are being used in targeted drug delivery and controlled drug release [8-10]. Researchers believed that these core-shell nanostructures can be used as a replacement of monometallic NPs in diverse applications. Particularly in biomedical field, some of major applications like bioimaging, cell levelling, and tissue engineering has already been developed and some of applications are at the innovation stage [11].

It is well known that among noble metal NPs Ag and Au are more recognised due to attractive physicochemical properties and biological functionalities and thus have been investigated repeatedly in different scientific areas [11-12]. AgNPs, in general are well known for their

* Corresponding Author Email: acharyadebashish0@gmail.com

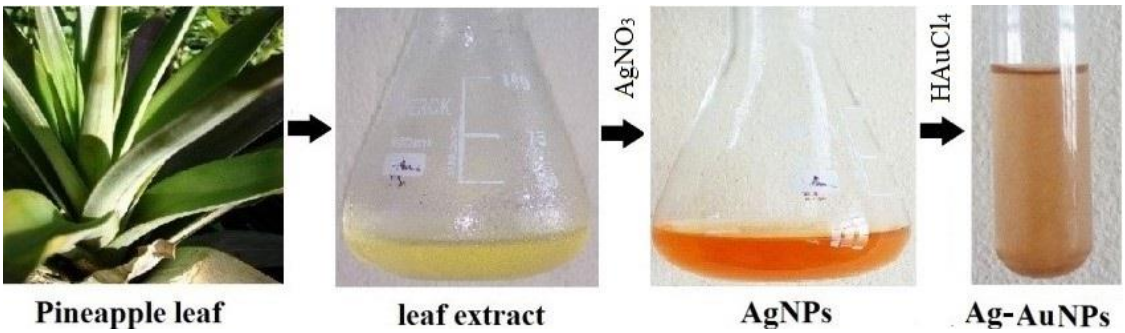

Fig. 1. Synthesis mechanism from pineapple leaf to Ag and Ag-Au core-shell NPs.

antimicrobial properties non-toxic to human while Au colloids have advantages of easy preparation, homogeneity and compatibility with biomolecules like antibody, antigen [13-14]. It has been reported that Ag and Au NPs either alone or in composite with polymer could also be used as antibacterial, antifungal and anticancer agents [14]. However, the antibacterial efficacy of bimetallic core–shell NPs containing Ag as core and Au as shell remains unexplored.

To date, several biogenic routes have been developed for the synthesis of Ag and Au NPs which simply involved the reduction of metal ions using biomolecules [13-15]. From traditional age to modern age entire part of Pineapple plant have been reported to provide vast medicinal benefits to human by curing ailments such as fungi, bacteria, tumour, flu, dysentery, diarrhea, diabetics, throat inflammation, tuberculosis, muscle cramp and cancer. Pineapple (*Ananas comosus L.*) an edible member of the botanical family Bromeliaceae of about two thousand species and also a subtropical fruit native to Philippines, Thailand, China and India. Its leaves are spiny, narrow, fibrous and the fruit grows on a stalk in the centre of rosette leaves. Besides fruits, pineapple leaves are being produced to yield a large amount of high-quality fibre which has been proved as a good substitute of synthetic fibres. Researchers found that the core, peel and crown extract of pineapple contains sugar especially fructose, sucrose and glucose. The biomolecules like vitamin B, vitamin C, Thiamine and riboflavin found in Pineapple are important micronutrients. These biomolecules contain carbonyl, hydroxyl and amine functional group which might be responsible for the reduction of metal ions to NPs [16]. Apparently, the same biomolecules also act as capping agent for the stabilization of newly formed particles during their growth process. Although reports are available for the synthesis of AgNPs using pineapple fruit [17-18] however, this study is the first report of Ag-Au NPs biosynthesis using pineapple leaf extract (Fig. 1).

MATERIALS AND METHODS

Collection of the plant materials

Healthy pineapple leaves were collected from the campus of Assam university, Assam, India.

Chemicals

Gold chloride ($HAuCl_4$) pure (49%) was purchased from SRL, India and silver nitrate ($AgNO_3$) from Fisher scientific, India. De-ionized water (DIW) was used for all reactions and laboratory purposes.

Microorganisms and Growth Conditions

Luria Bertani (LB), and nutrient medium (NM) and constituents of growth media were purchased from HI Media, India. *E. coli* ATCC 25922 and *S. aureus* ATCC 25923 are type strains which were taken from culture collection of the Department of Microbiology, Assam University. The bacterial strains were grown on LB or NM as per the requirements, and stored on nutrient agar (NA) slants at -20 °C. The cultures were revived on LB broth and sub-cultured after regular intervals.

Preparation of leaf extract

About 18g of Pineapple leaves were taken and washed 2-3 times by DIW to remove dust and unwanted visible particle, finely chopped and blended. 50 mL DIW was added to the blended mass and was heated at 80^0C for 30 min. The extract was filtered with no.1 Whatman filter paper and the filtered solution was stored at 4^0C for further use.

Synthesis of AgNPs

In a typical experiment, 5 mg of $AgNO_3$ was dissolved in 5 mL of DIW and the solution was then added to 20 mL of pineapple leaf extract under constant stirring (200-300 r/min) at room temperature (27^0C). Color change of the resultant mixture from light yellow to reddish yellow was noted after about 10-20 min indicating the formation of AgNPs.

Synthesis of bimetallic Ag-Au core-shell NPs

10 mL of freshly prepared AgNPs solution was taken and washed 2 to 3 times with DIW and centrifuged at 5000 r/min for 10 min to remove excess absorbed substance on the surface of AgNP. To the solution, 400 µL of $HAuCl_4$ (0.4mM) was added drop wise while maintaining constant stirring at room temperature (27^0 C). The color change from reddish yellow to light brown was observed within 15-20 min suggesting the formation of Ag-Au core-shell NPs (scheme 1). The overall synthesis procedure was protected from light.

Characterization Techniques

Physical and chemical characterisation of the synthesized Ag and Ag-Au core-shell NPs were performed using various analytical techniques. The bio-reduction of metal ions and the formation of NPs in aqueous solution were monitored by UV-Vis spectrophotometry (Perkin Elmer, Lambda 25, US) by scanning the absorbance ranging from 300 to 800 nm at a resolution of 1 nm. The chemical composition and functional groups of NPs were determined using FTIR (Perkin Elmer Spectrum 2, US) analysis was carried out. Crystalline phase and structural properties of NPs were analysed by XRD (Rigaku Corporation, Miniflex spectrometer, Japan) by taking small amount of solution and drying it on a quartz plate with CuKα radiation (λ = 1.54056 Å). Finally, surface morphology and size distribution of NPs were investigated by TEM (JEOL JEM 2100, Japan) operated at 200 kV. The samples for TEM analysis were prepared by placing a drop of homogeneous suspension on a copper grid film and allowing it to dry at room temperature.

Purification of NPs

The purification of prepared NPs was performed by centrifugation at 10000 r/min for 20 min at 27^0C (Remi R8C, Remi, Mumbai, India) and a dried powder of the nanosized Ag and Ag-Au was obtained by freeze-dying process as discussed by Abdelwahed *et al.* [19]. Further, prepared pellets were washed 3 to 4 times with DIW and centrifuged at 10000 r/min for 15 min to remove excess ions. The re-suspended aqueous homogenate of both NPs was diluted for different trials. Original concentrations of stock solution, and dilution factors were considered for the determination of concentrations of both typed NPs [20].

Antibacterial activity

Bacterial sensitivity to antibiotics is commonly tested using disc diffusion test, employing antibiotic impregnated disk [20]. A similar test with NP laden disc was used to evaluate the bacterial sensitivity towards AgNPs, as marked by their zone of inhibition (ZOI). 5 mL of bacterial suspension were applied uniformly on the surface of NA plate. Immediately afterwards, small disc of uniform size (± 5 mm diameter) containing Ag and Ag-Au core-shell NPs of 706, 692, 673, and 642 µg/mL designated as B1, B2, B3 and B4 respectively were placed carefully on the plates. After 24 h of incubation, the plates were examined for ZOI and the diameters of zones were recorded.

RESULT AND DISCUSSION

UV-Visible spectroscopy

The initial characterisation of Ag and Ag-Au core-shell NPs was performed using UV–Vis spectrometer at various reaction times shown in Fig. 2. The reduction of Ag^+ to Ag^0 and Au^{3+} to Au^0 was confirmed by color change of the reaction mixture from light yellow to light brown. This color change is morphological indicator to detect the synthesis of metal NPs and this could be attributed to surface plasmon resonance (SPR) arising due to the collective oscillation of free conduction electrons induced by an interacting electromagnetic field [21]. For smaller metal NPs (< 30 nm), SPR appears at shorter wavelength while for larger particles (> 30 nm) SPR shifts to longer wavelength. Moreover, SPR of metal NPs strongly depends on the shape and local refractive index of surrounding medium. The formation of AgNPs was confirmed by the SPR peak at 442 nm which appeared at interval 10-20 min after the addition of $AgNO_3$ to leaf extract. A continuous increase in the intensity of the peaks was observed from first 5 to 20 min with little variation in the absorption maxima. 20 min after the addition of $HAuCl_4$ to the AgNP solution, a decrease in the intensity of the

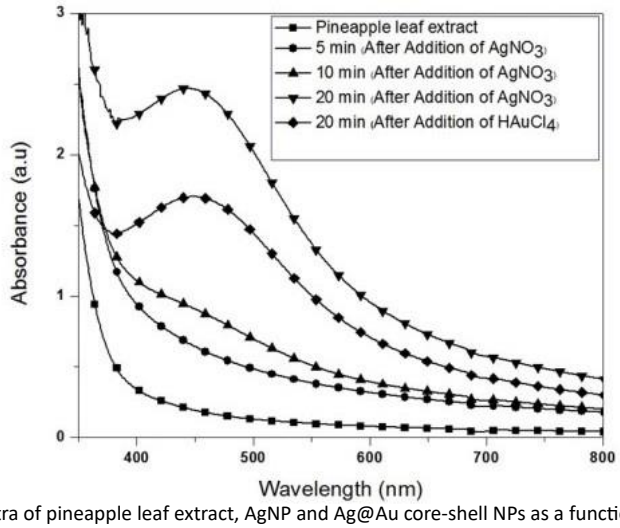

Fig. 2. UV-Vis spectra of pineapple leaf extract, AgNP and Ag@Au core-shell NPs as a function of reaction time.

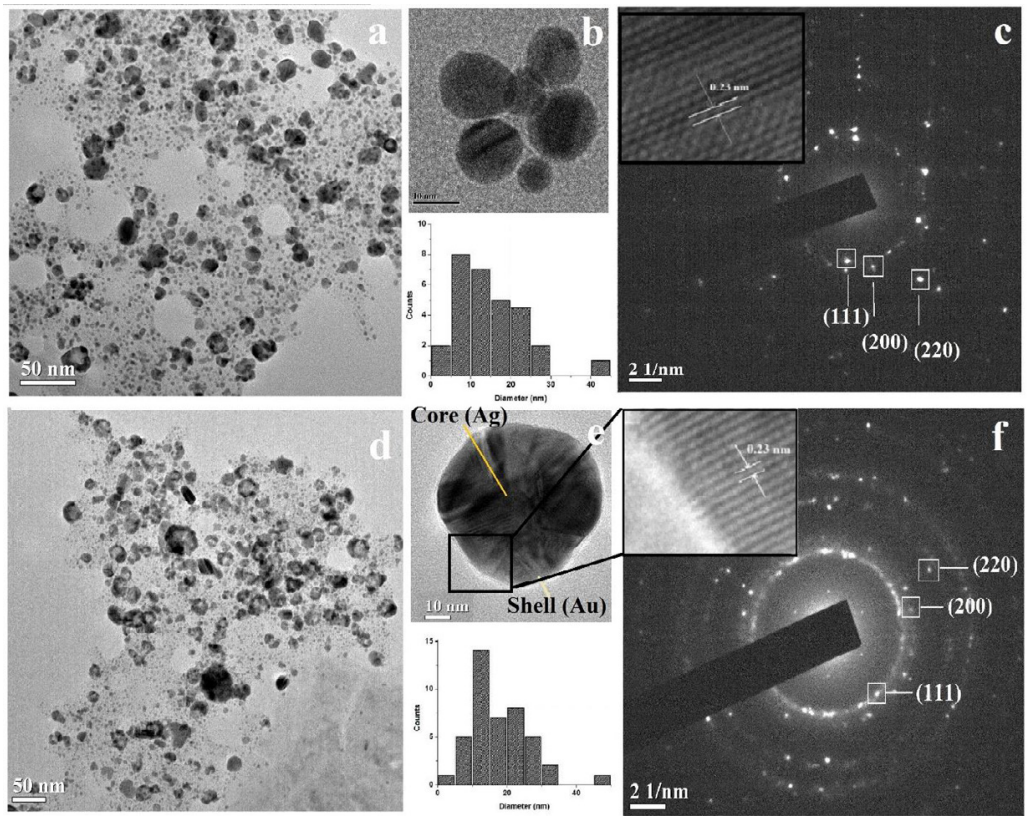

Fig. 3. TEM, HRTEM (inset), size distribution, SAED pattern and lattice spacing (inset) of (a, b, c) AgNPs and (d, e, f) Ag-Au core-shell NPs.

peaks was observed with slight redshift (at 452 nm) in the absorption maxima. The redshift observed was due to the coating of Au shell around Ag core which increased the local refractive index of the surrounding medium [22].

TEM analysis

Morphology and size distributions of the synthesized NPs were determined from TEM images and shown in Fig. 3 (a, b, d and e). The particles formed were spherical in shape. The size

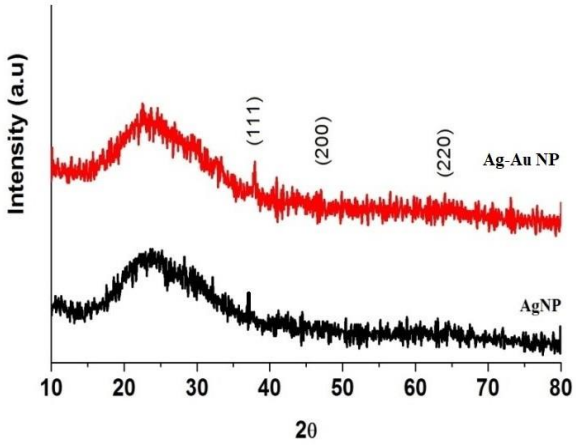

Fig. 4. XRD spectra of Ag and Ag-Au core-shell NPs.

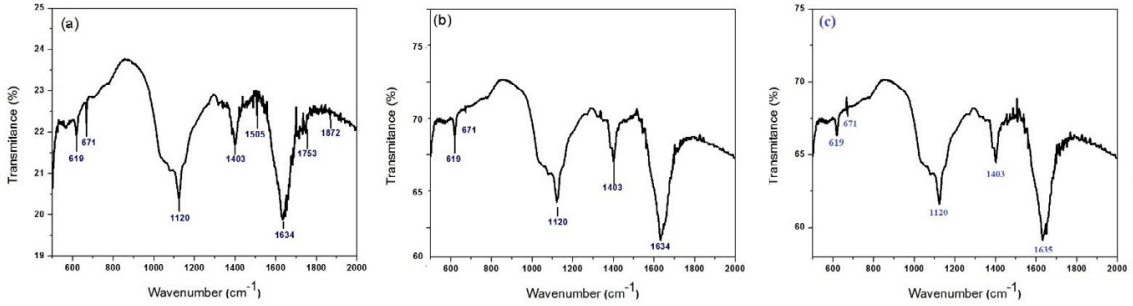

Fig. 5. IR spectra of (a) pineapple leaf extract, (b) AgNPs and (c) Ag-Au core-shell NPs.

range of AgNPs was estimated at 5-25 nm with average size 10 nm while Ag-Au NPs were found in the ranges 5-30 nm in size, with average core size 12 nm and shell thickness 5 nm. Lattice spacing for both samples were found as 0.23 nm (inset Fig. 3 (c, f)) which corresponds to plane (111) (JCPDS file No: 02-1098 and 01-1172). The planes (111), (200) and (220) obtained from SAED pattern confirmed the crystalline nature of NPs (Fig. 3 (c, f)). Some incomplete shell formation around silver core were also observed which could be due to the rapid reduction of Au ions over Ag core [22-23].

XRD analysis

XRD pattern of Ag and Ag-Au NPs are shown in Fig. 4. The crystallographic data obtained from XRD analysis revealed that both the samples were of face cubic centre (fcc) structured. The prominent peak appeared for AgNPs at 2=38.10^0, 45.06^0 and 63^0 corresponds to (111), (200) and (220) plane (JCPDS file No. 01-1167) and those for Ag-Au NPs was 38^0 corresponds to (111) plane. Earlier, it was reported that Ag and Au NPs having (111) plane contains high atomic density of electrons and are known to be very reactive [24]. Herein, antibacterial activities of both samples were studied against two different bacteria which can be ascribed to the interaction of bacterial surface with (111) planes of AgNPs resulted in disruption of cell structure [20, 24].

FTIR study

Functional groups responsible for the bio-reduction, capping and stabilizing of NPs were analyzed using FTIR. The IR spectra of pineapple leaf extract, AgNPs and Ag-Au NPs are shown in Fig. 5 (a, b, c) respectively. The IR spectrum of pineapple leaf extract showed different major peak positions at 619, 671, 1120, 1403, 1505, 1634, 1753 and 1872 cm^{-1} (Fig. 5a). Almost similar absorption peaks were observed in the spectra of Ag and Ag-Au NPs. The broad peaks appeared at 619 and 671 cm^{-1} of leaf extract, AgNPs and Ag-Au NPs could be assigned to –CºC–H: C–H bending vibration of alkynes group while the peak

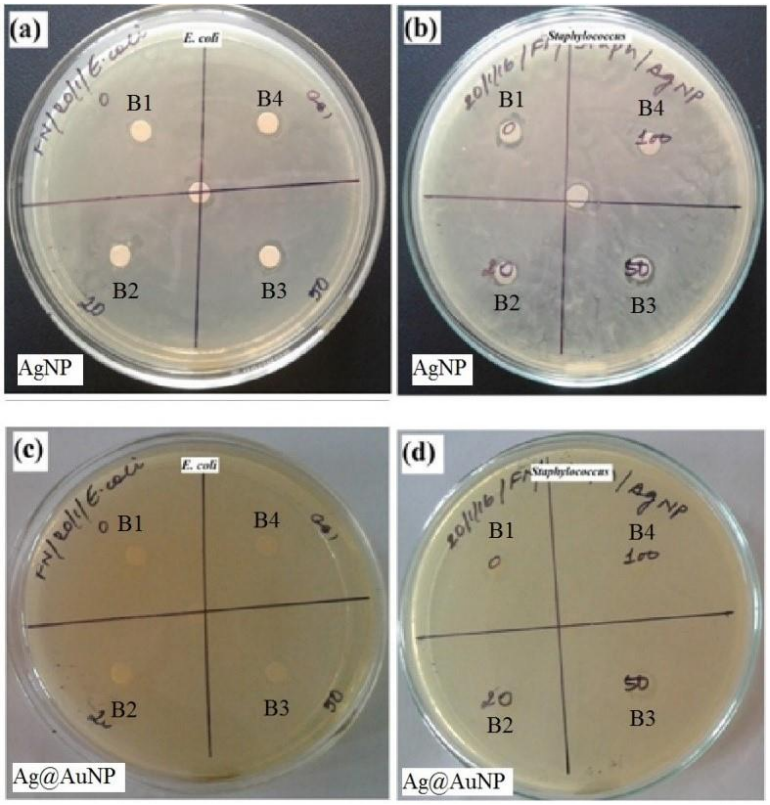

Fig. 6. Disc diffusion test of (a, b) AgNPs and (c, d) Ag-Au core-shell NPs at different concentrations against *E. coli* and *S. aureus*.

at 1120 cm^{-1} represents C–N stretching vibrations of aliphatic amines group. The peaks appeared at 1403 and 1634 cm^{-1} were assigned to C–H bending vibration of alkanes group while peak at 1753 cm^{-1} was attributed to C=O stretching vibration in carbonyl group. The other peak at 1505 cm^{-1} could be assigned to C–C stretching of aromatics group. Here, comparing the three spectra, there was no free C–C and C=O found in the NPs spectra (Fig. 5 b, c) against the peaks at 1505 and 1753 cm^{-1} in leaf extract spectra (Fig. 5a) indicating carbonyl and aromatics group may be involved as capping and stabilizing agents of Ag and Ag-Au NPs. Similar results had been reported by Emeka and Ahmad co-workers [15, 18]. They also added that biomolecules with amine, carbonyl and hydroxyl groups in pineapple leaf acted as a metal ion reducing and capping agent in the newly formed NPs during their growth processes.

Antibacterial study

The antibacterial potential of the synthesized NPs against clinical organisms *S. aureus* and *E. coli* were investigated using four different concentrations, respectively (642 µg/mL, 673 µg/mL, 692 µg/mL and 706 µg/mL) and shown in Fig. 6 (a, b, c, d) and Table 1. All the concentrations (642-706 µg/mL) of AgNPs and Ag-Au NPs were found to be effective against *E. coli* while concentration of 673, 692 and 706 µg/mL was found significant against *S. aureus*. Previously, the antibacterial activities of various metallic NPs were tested by various research groups against both Gram-positive and Gram-negative pathogens [25-27] but Ag-Au core-shell NPs as bactericidal agents have not yet been reported. As per literature, smaller sized AgNPs interact with the bacterial membrane and causes cell damages. Some antibacterial reports also emphasized on the role of Ag ions with negatively charged bacterial cell wall which interacts with DNA, protein and sulfur constituents that ultimately leads to cell death [28-30]. Similar to previous work, herein we assume Ag ions released in the bacterial suspension or direct contact with bacterial cell wall is responsible for antibacterial effect.

Table 1. Zone of inhibition (mm) against various microorganisms at different concentrations (mg/mL) of AgNPs and Ag-Au core-shell NPs.

Label	Conc. (µg/mL)	*E. coli*		*S. aureus*	
		AgNP	Ag-Au NP	AgNP	Ag-Au NP
B1	706	8	6.25	8.5	8.23
B2	692	7.2	6.33	6.3	6.92
B3	673	9.2	6.70	8	8.18
B4	642	8.2	7	No zone	No zone

CONCLUSION

Ag and Ag-Au core-shell NPs were successfully synthesized by a rapid, ecofriendly and cost-effective greener approach. The NPs were characterized by UV-Vis spectroscopy, FTIR, XRD and TEM analyses confirming the formation spherical shaped NPs. The average sizes were obtained as ~ 10 nm for AgNPs and ~ 12 nm for Ag-Au core-shell NPs respectively. On disc diffusion test, both the NPs were found to be suitable antibacterial candidates against pathogenic microbes. Thus, it can be concluded that present synthesis route will be useful in the development of similar stable systems with other metal NPs and in future these greener core-shell NPs could be used as advanced nanomaterials for other applications like catalysis, fuel cell, gene delivery.

ACKNOWLEDGMENT

The authors gratefully acknowledge UGC for proving funds through SAP program for procuring analytical instruments UV-visible spectrophotometer, FTIR. The authors also would like to acknowledge SAIF NEHU, Shillong, India for providing TEM facility and Manipur University, India for XRD facility.

CONFLICT OF INTEREST

The authors declare that there is no conflict of interest.

REFERENCES

[1] Shanmuganathan R., Lewis Oscarb F., Shanmugamc S., Thajuddind N., Alharbie S. A., Alharbie N. S., Brindhadevif K., Pugazhendhif A., (2020), Core/shell nanoparticles: Synthesis, investigation of antimicrobial potential and photocatalytic degradation of Rhodamine B. *J. Photochem. Photobio. B.* 202: 111729-111735.

[2] Saravanan M., Arokiyaraj S., Lakshmi T., Pugazhendhi A., (2018), Synthesis of silver nanoparticles from Phenerochaete chrysosporium (MTCC-787) and their antibacterial activity against human pathogenic bacteria. *Microbial Patho.* 117: 68-72.

[3] Pugazhendhi A., Prabakar D., Jacob J. M., Karuppusamy I., Saratale R. G., (2018), Synthesis and characterization of silver nanoparticles using Gelidium amansii and its antimicrobial property against various pathogenic bacteria. *Microbial Patho.* 114: 41-45.

[4] Folorunso A., Akintelu S., Oyebamiji A. K., Ajayi S., Abiola B., Abdusalam I., Morakinyo A., (2019), Biosynthesis, characterization and antimicrobial activity of gold nanoparticles from leaf extracts of Annona muricate. *J. Nanostruct. Chem.* 9:111–117.

[5] Pugazhendhi A., Edison T. N. J., Karuppusamy I., Kathirvel B., (2018), Inorganic nanoparticles: A potential cancer therapy for human welfare. *J. Pharma.* 539: 104-111.

[6] Baghayeri M., Veisi H., Veisi M. N., (2018), Designing and fabrication of a novel gold nanocomposite structure: Application in electrochemical sensing of bisphenol. *J. Environ. Anal. Chem.* 98: 874-888.

[7] Ghanei-Motlagh M., Baghayeri M., (2020), Determination of trace Tl (I) by differential pulse anodic stripping voltammetry using a novel modified carbon paste electrode. *J. Electrochem. Soc*. 167: 066508-066516.

[8] Nodehi M., Baghayeri M., Ansari R., Veisi H., (2020), Electrochemical quantification of 17α – Ethinylestradiol in biological samples using a Au/Fe O @TA/MWNT/GCE sensor. *Mat. Chem. Phy.* 244: 122687-122698.

[9] Thakur S., Thakur S., Kumar R., (2018), Bio-nanotechnology and its role in agriculture and food industry. *J. Mol. Genet. Med*. 12: 1-9.

[10] Jain S., Mehata M., (2018), Pure flavonoid mediated green synthesis of silver nanoparticles and their enhanced antibacterial property. *Scientif. Rep.* 7: 1586-1599.

[11] Chen D., Li C., Liu H., Ye F., Yang J., (2015), Core-shell Au@Pd nanoparticles with enhanced catalytic activity for oxygen reduction reaction via core-shell Au@Ag/Pd constructions. *Scientif. Rep*. 5: 11949-11955.

[12] Calagua A., Alarcon H., Paraguay F., Rodriguez J., (2015), Synthesis and characterization of bi-metallic gold-silver core-shell nanoparticles: a green approach. *Adv. Nanopart.* 4: 116-121.

[13] Khatami M., Alijani H Q., Sharifi I., (2018), Biosynthesis of bimetallic and core–shell nanoparticles: Their biomedical applications. *IET Nanobiotechnol*. 12: 879 – 887.

[14] Khalil M. M. H., Sabry D. Y., Mahdi H., (2017), Green synthesis of silver, gold and silver-gold nanoparticles: Characterization, antimicrobial activity and cytotoxicity. *J.*

Sci. Rea. Sci. 34: 553-574.

[15] Elemike E. E., Onwudiwe D. C., Fayemi O. E., Botha T. L., (2019), Green synthesis and electrochemistry of Ag, Au, and Ag–Au bimetallic nanoparticles using golden rod (*Solidago canadensis*) leaf extract. *Appl. Phy. A*. 125: 1-12

[16] Asim M., Abdan K., Jawaid M., Nasir M., Dashtizadeh Z., Ishak M.R., Enamul H., (2015), A Review on Pineapple Leaves Fibre and Its Composites. *Int. J. Polymer Sci.* 2015: 1-16.

[17] Emeka E. E., Ojiefoh O. C., Aleruchi C., Hassan L. A., Christiana O. M., Rebecca M., Dare E. O., Temitope A. E., (2014), Evaluation of antibacterial activities of silver nanoparticles green-synthesized using pineapple leaf (*Ananas comosus*). *Micron*. 57: 1-5.

[18] Ahmad N., Sharma S., (2012), Green synthesis of Silver nanoparticles using extracts of *Ananas comosus*. *Green Sustain. Chem.* 2: 141-147.

[19] Abdelwahed W., Ghania Degobert G., Stainmesse S., Fessi H., (2006), Freeze-drying of nanoparticles: Formulation, process and storage considerations. *Adv. Drug Delivery Rev*. 58: 1688–1713.

[20] Ruparelia J. P., Chatterjee A. K., Duttagupta S. P., Mukherji S., (2008), Strain specificity in antimicrobial activity of silver and copper nanoparticles. *Acta Biomaterialia.* 4: 707-7016.

[21] Mulvaney P., Giersig M., Henglein A., (1992), Surface chemistry of colloidal gold: Deposition of lead and accompanying optical effects. *J. Phys. Chem*. 96: 10419–10424.

[22] Sangaru S. S., Rai A., Ahmada A., Sastry M., (2004), Rapid synthesis of Au, Ag, and bimetallic Au core-Ag shell nanoparticles using Neem (*Azadirachta indica*) leaf broth. *J. Colloid Interf. Sci*. 275: 496-502.

[23] Chaudhuri R. G., Paria S., (2012), Core/shell nanoparticles: Classes, properties, synthesis mechanisms, characterization, and applications. *Chem. Rev.* 112: 2373–2433.

[24] Acharya D., Singha K. M., Pandey P., Mohanta B., Jina R., Singha L. P., (2018), Shape dependent physical mutilation and lethal effects of silver nanoparticles on bacteria. *Scientif. Rep.* 8: 201-212.

[25] Agnihotri S., Mukherji S., (2014), Size-controlled silver nano-particles synthesized over the range 5–100 nm using the same protocol and their antibacterial efficacy. *RSC Adv*. 4: 3974–3983.

[26] Ghaffari-Monghaddam M., Eslahi H., (2014), Synthesis, characterization and antibacterial properties of a novel composites based on polyaniline/polyvinyl alcohol/Ag. *Arabian J. Chem.* 7: 846–855.

[27] Nahar K., Aziz S., Bashar M. S., Md. Haque A., Al-Reza S., (2020), Synthesis and characterization of Silver nanoparticles from *Cinnamomum tamala* leaf extract and its antibacterial potential. *Int. J. Nano Dimens*. 11: 88-98.

[28] Daphedar A., Ritti M., Patil N., Patil S., Kakkalameli S., Taranath T. C., (2020), Synthesis and characterization of Silver nanoparticles from fruit extract of *Michelia Champaca L*.: Their antioxidant and antibacterial activity. *Int. J. Nano Dimens*. 11: 267-276.

[29] Sadeghi B., Gholamhoseinpoor F., (2015), A study on the stability and green synthesis of silver nanoparticles using *Ziziphora tenuior* (Zt) extract at room temperature. *Spectrochim. Acta Part A-Mol. Biomol. Spectros.*134: 310–315.

[30] Sadeghi B., Rostamib A., Momeni S. S., (2015), Facile green synthesis of silver nanoparticles using seed aqueous extract of *Pistacia atlantica* and its antibacterial activity. *Spectrochim. Acta Part A-Mol. Biomol. Spectros.* 134: 326-332.